IEEE P802.15
Wireless Personal Area Networks

Project	IEEE P802.15 Working Group for Wireless Personal Area Networks (WPANs)	
Title	**Statistical 60 GHz Indoor Channel Model Using Circular Polarized Antennas**	
Date Submitted	[7 November 2006]	
Source	[Zhiguo Lai, University of Massachusetts] [Abbie Mathew, NewLANS] [Salvador Rivera, NewLANS] [Dev Gupta, NewLANS]	[zhlai@ece.umass.edu] [amathew@newlans.com] [srivera@newlans.com] [dgupta@newlans.com]
Re:	[]	
Abstract	[This paper describes a statistical 60 GHz indoor channel model with circular polarized antennas, which includes time-of-arrival (ToA) and angle-of-arrival (AoA) characteristics. A time-domain measurement system that was used to simultaneously collect the temporal and spatial data is described. Data processing methods are outlined, and results obtained from data taken in office and residential environments are presented.]	
Purpose	[]	
Notice	This document has been prepared to assist the IEEE P802.15. It is offered as a basis for discussion and is not binding on the contributing individual(s) or organization(s). The material in this document is subject to change in form and content after further study. The contributor(s) reserve(s) the right to add, amend or withdraw material contained herein.	
Release	The contributor acknowledges and accepts that this contribution becomes the property of IEEE and may be made publicly available by P802.15.	

Statistical 60 GHz Indoor Channel Model Using Circular Polarized Antennas

Zhiguo Lai [¶], Abbie Mathew [¶¶], Salvador Rivera [¶¶], and Dev Gupta [¶¶]

[¶] University of Massachusetts, Amherst, MA 01003, USA
[¶¶] NewLANS Company Inc., Acton, MA 01720, USA
Emails: zhlai@ece.umass.edu; {amathew, srivera, dgupta}@newlans.com

Abstract: In this paper, a statistical 60 GHz indoor channel model, which includes time-of-arrival (ToA) and angle-of-arrival (AoA) characteristics, is proposed based on a measurement campaign using circular polarized antennas. A time-domain measurement system that was used to simultaneously collect the temporal and spatial data is described. Data processing methods are outlined, and results obtained from data taken in two different environments are presented.

1. Introduction

In high speed indoor radio communications systems, delay distortion due to multipath components (MPCs) is a serious cause of channel degradation. Circular polarized signals have the property of reducing MPCs. This has been reported in the work done by a number of researchers in this area [1-3]. However almost all the existing statistical models are based on linear polarized antennas. Specifically, the work done by Manabe and Sato [2] provides interesting results. Their work showed that the root-mean-square (RMS) delay spread with right hand polarization is about half that of vertical and horizontal polarizations. They also reported that circular polarization reduced MPCs up to 30 dB with respect to the linear polarizations. They then conducted experiments to determine a relationship between polarization and bit error rate (BER). For a 150 Mbps BPSK transmission with an SNR of 15 dB, the BER with circular polarization was significantly lower than that with linear polarizations. The authors of this paper are not aware of papers describing 60 GHz channel model with circular polarized signals.

Motivated by this, University of Massachusetts and NewLANS undertook a 60 GHz indoor measurement campaign to support the IEEE 802.15.3c task group in the development of a wireless personal area network (WPAN) standard. The objective of the campaign was to develop a statistical channel model for circular polarized pulse transmission in support of applications in office and residential environments. The data acquisition system developed for this measurement campaign is capable of resolving MPC arrivals simultaneously in time and space domains. The system was used to collect a number of data sets from these two environments. This paper reports the results of these measurements, and then proposes a statistical model which includes both time-of-arrival (ToA) and angle-of-arrival (AoA) characteristics of the indoor channel.

Most of the temporal-spatial channel models proposed so far made the assumption that the statistics for the ToA and the AoA are independent. To the best of the authors' knowledge, the first thorough investigation (and probably the only one available in the literature) on the temporal-spatial correlation in indoor propagation environments based on real measurement data was that of Chong, *et. al.* [4], although Spencer *et. al.* [5] contained a brief discussion on this

issue. In this paper, a joint probability distribution function (PDF) for the ToA and the AoA is presented following the approach described in [4].

The organization of the paper is as follows. Section 2 describes the measurement setup and environments. Section 3 presents the technique used to extract MPC ToA and AoA information from the measured data. A new statistical channel model is proposed in Section 4, followed by a discussion of parameters in Section 5. Finally, appropriate conclusions are drawn in Section 6.

2. Measurement Setup and Environments

2.1 Measurement Setup

The measurements were made in time-domain such that reflections and impulse responses are available almost instantaneously. A block diagram of the system is shown in Figure 1. The pulse generator modulates the 61.6 GHz from the dielectric resonator oscillator (DRO) to create a 1 ns pulsed signal. The receiver down converts the received signal to an intermediate frequency (IF) of 5.4 GHz. The pulsed data is recorded using an Agilent 86100A digital storage oscilloscope connected to a laptop computer, which captures the information displayed by the scope and saves the data in an Excel spreadsheet. At the start of each measurement, the transmitter and the receiver were bore sighted. The basic technique used to collect the data involved pointing the receiver in a certain direction, measuring the time-domain impulse response (from the IF output) of the channel in that direction, rotating the receiver a small amount (about 2°) with the transmitter fixed, and repeating the procedure until full 360° coverage was obtained. Measurements were taken at each increment. The transmitter and receiver antennas, both right hand polarized, have a half power beam width (HPBW) of 35° and 13° respectively.

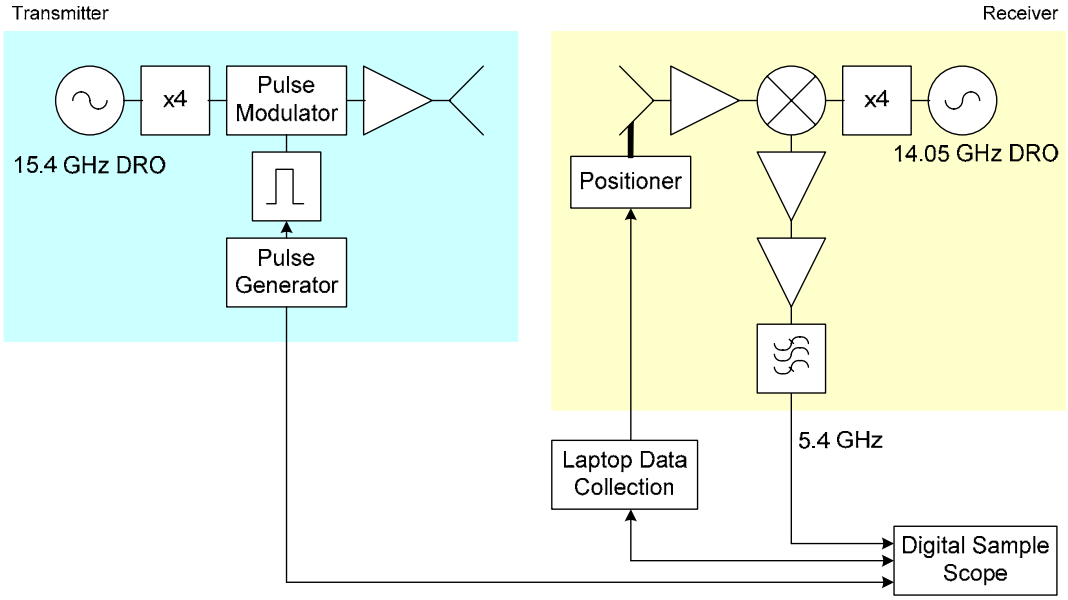

Figure 1. Measurement setup

2.2 Environments

Office and residential environments were considered in the measurement campaign. The office environment consisted of cubicles, conference rooms, and hallway/corridor. Each of them comprised of following articles:

- Office cubicles: metal shelves, white boards, and office windows
- Conference rooms: metal shelves, white boards, and office windows
- Hallway/corridor: office cubicles, metal shelves, and walls

The residential measurements were made in US homes and they consisted of living/family rooms, dining rooms, and kitchen. The environments consisted of windows, doors, picture frames, wooden furniture, and fire place. Table 1 summarizes the number of measurements taken in each environment and Figures 2 shows the layouts of some locations considered in the campaign.

Table 1. Number of measurement points in the campaign

Environment	Number of Locations	Number of Measurements
Office	33	6,006
Residential	30	5,460
	63	11,466

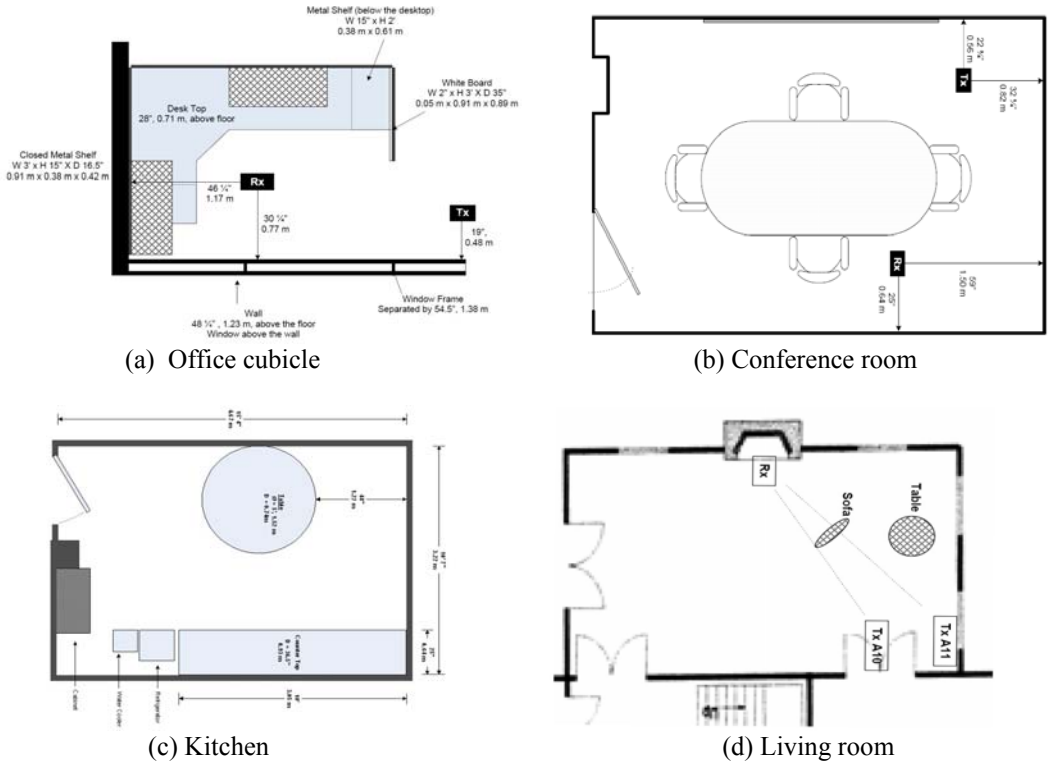

(a) Office cubicle (b) Conference room

(c) Kitchen (d) Living room

Figure 2. Sketch layouts of some locations considered in the measurement campaign

3. Data Processing and Analysis

3.1 Baseband Pulse Recovery

As mentioned in the previous sections, time-domain impulse responses were measured as the receiver rotated through 360°. The response at each angle is an IF signal centered at about 5.4 GHz. An envelope detector was digitally implemented in Matlab to recover the baseband pulses:

- The response was first bandpass filtered at 5.4±1.0 GHz.
- The envelope of the output was obtained through Hilbert transform [6].
- Baseband pulses were recovered after lowpassing the envelope (cutoff of 1.0 GHz).

3.2 Image Processing

Data produced by this procedure can best be viewed in the form of an image plot of the normalized received power (with respect to the LOS signal) as a function of time and angle. An example of such plots is shown in Figure 3a. This data set was taken from cubicle measurements (Figure 2a), where the transmitter and receiver separation is about 1.8 m. Note that in his figure, the vertical axis represents the absolute delay from the transmitter. Also note that a -30 dB threshold has been applied. From this image plot, one can clearly see the signal due to LOS path (zero angle) as well as two reflections at large angles.

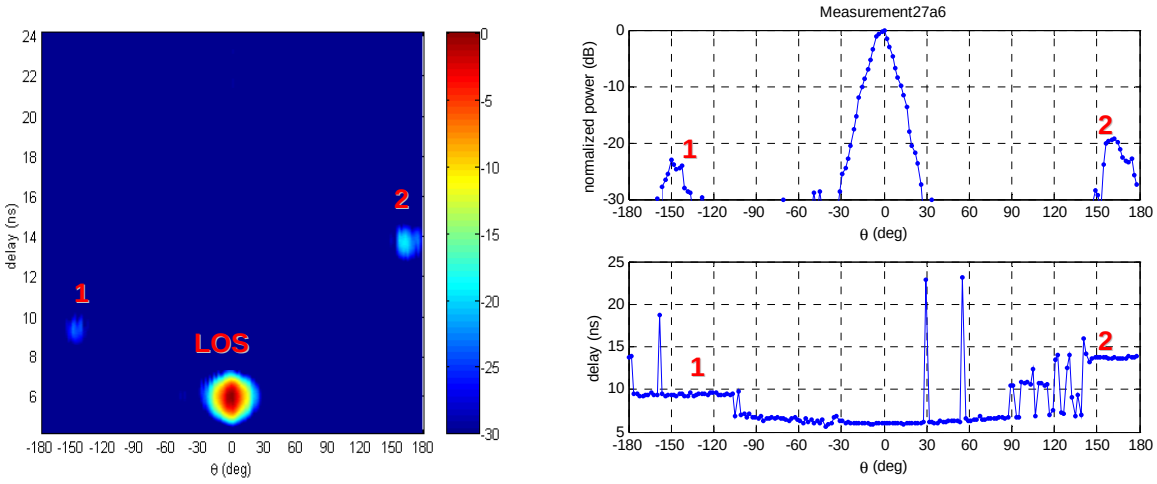

(a) Image plot (b) Reflection plot

Figure 3. Example of a processed data set.

Computer algorithms, such as CLEAN and KDE, are available to extract MPC information (power, ToA, and AoA). However these algorithms are usually time-consuming and they tend to pick up false detections which may need to be manually removed. We had made accurate layout diagrams for each location during the measurement campaign. Due to the simplicity of the measured data, MPC information in our data sets was manually collected from processed data along with the help of environment layouts.

Consider the example given in Figure 3a, which is the reflection measurement of the office environment in Figure 2a. To accurately determine the MPC information, the peak value and its corresponding delay of the received power at each angle were plotted in Figure 3b. Looking at the layout diagram and the reflection plot, one can determine that the true reflections, not the anomalies of the antenna integrating reflected power, were captured. One can further determine that 1 and 2 are single ray reflections (from the metal shelf and the wall behind the receiver respectively). The image plot and the reflection plot in Figure 3, confirmed the selection. This procedure was used for all the measurements.

3.3 Antenna Deconvolution

The antenna deconvolution process was carried out by a process explained in the previous paragraph. This was made possible as only a few scattered MPCs were observed in each of the measurements. This was facilitated by the -30 dB threshold. The 13° HPBW receiver antenna and circular polarization further reduced multipath reflections.

4. Proposed Statistical Indoor Channel Model

In this section we propose a statistical model for the indoor multipath channel that includes a single-cluster version of the S–V model [7] and incorporates spatial information. Model parameters are derived from the data collected during the measurement campaign described in Section 2. By assuming a finite number of MPCs (since a proper threshold has been applied), the channel impulse response (CIR) can be expressed as

$$h(t,\theta)=\beta\left[\delta(t-t_{\mathrm{LOS}},\theta)+\sum_{l=1}^{L}\alpha_l\delta(t-t_{\mathrm{LOS}}-t_l,\theta-\theta_l)\right] \quad (1)$$

where $\delta(\cdot)$ is the Dirac delta function, β is a normalization factor that can be determined from the measurement setup (e.g., the free-space path loss, transmitter and receiver gains, etc.), t_{LOS} is the absolute delay corresponding to the LOS path, L is the number of rays, α_l, t_l, and θ_l are the amplitude, the ToA, and the AoA of the l-th ray, respectively. Notice that the last three parameters are all relative values with respect to the LOS signal.

5. Extraction of Channel Parameters

This section presents the statistical characterization of channel parameters defined in the previous section. The variations of these parameters may be characterized statistically by fitting the measurement data against the proposed theoretical distributions.

5.1 Joint Distribution of the ToA and the AoA

Figure 4 shows the scatter plots of the ToA versus the AoA for office and residential environments. It can be seen that for both environments the ToA and the AoA are strong related. Roughly speaking, rays arriving at the receiver with shorter (or longer) delays tend to have relatively smaller (or larger) AoAs. Also it appears that there are no arrivals within ±10° of the LOS direction for the office environment and ±20° for the residential environment.

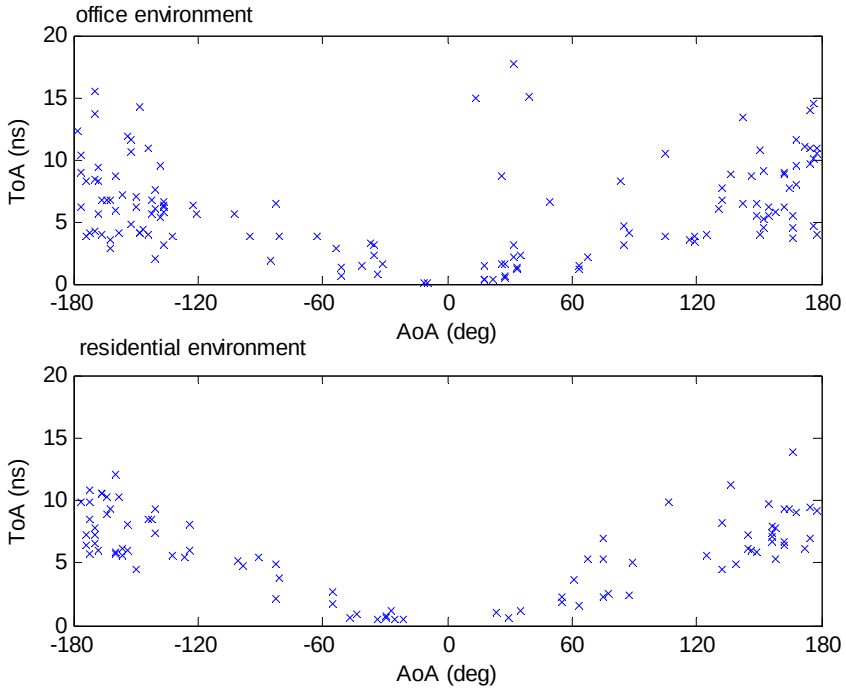

Figure 4. Scatter plots of the ToA versus the AoA for office and residential environments.

To better model the temporal-spatial property of the multipath channel, it is desirable to study the joint PDF between the ToA and the AoA, $f(t_l, \theta_l)$, which, following the approach described in [4], can be expressed as

$$f(t_l, \theta_l) = f(\theta_l \mid t_l) \cdot f(t_l) \tag{2}$$

where $f(\theta_l|t_l)$ is the conditional AoA PDF and $f(t_l)$ is the marginal ToA PDF.

The marginal ToA PDF, $f(t_l)$, was estimated by accumulating all rays' AoAs and is usually modeled by a Poisson process [7]:

$$f(t_l \mid t_{l-1}) = \lambda \cdot \exp\left[-\lambda(t_l - t_{l-1})\right], \quad t_{l-1} < t_l < \infty \tag{3}$$

where λ is the mean ray arrival rate. Figure 5 shows the marginal ToA histograms for both office and residential environments with their estimated PDFs plotted as solid curves. The estimated parameter from the measured data was $1/\lambda$ = 2.11 ns for the office environment and 2.29 ns for the residential environment.

Figure 6 shows the joint histograms for the ToA and the AoA. Note that the angular axis in this figure spans from 0° to 360° instead of from -180° to 180° considering the fact that the majority of arrivals are from the vicinity of ±180° except for extremely short delays. In [4], the conditional AoA PDF, $f(\theta_l|t_l)$, is associated with a set of so-called partial conditional AoA PDFs, $\{f(\theta_l|\tau_n), n = 0, 1, \cdots, N\text{-}1\}$, as follows:

$$f(\theta_l \mid t_l) = \sum_{n=0}^{N-1} f(\theta_l \mid \tau_n), \quad n \in \{0,1,\cdots,N-1\} \tag{4}$$

where $\tau_n = n\Delta\tau$ with $\Delta\tau$ being the delay step size and N the number of delay steps. Here $\Delta\tau$ = 2 ns was chosen in order to ensure that the number of rays within each delay step, K_n, was sufficient

(e.g., at least 20) for further statistical analysis of $f(\theta_l|\tau_n)$. By observing the shape of $f(\theta_l|\tau_n)$, a known PDF is proposed to represent the varying shape of $f(\theta_l|\tau_n)$ by a change of its parameter values (usually the mean and standard deviation).

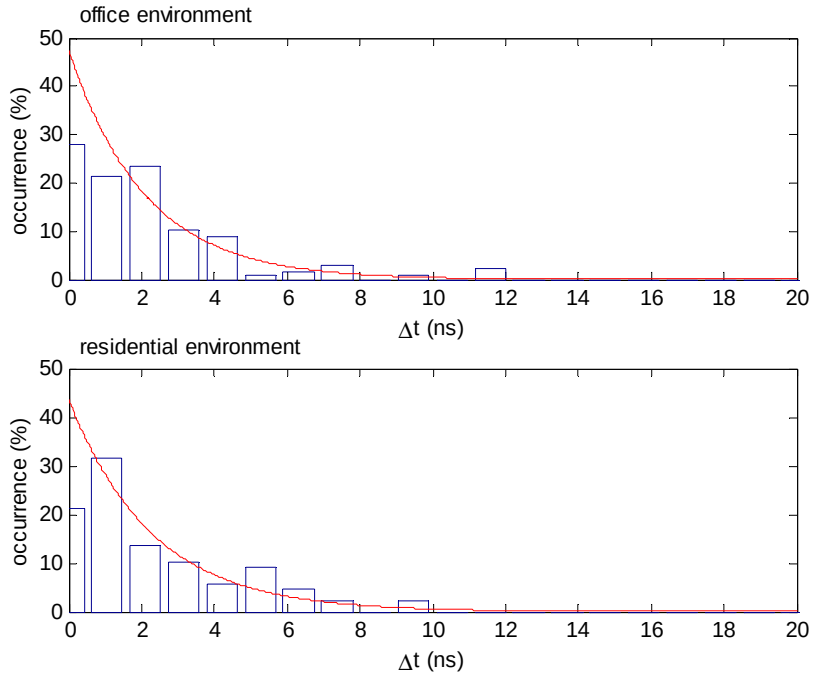

Figure 5. Marginal ToA PDFs for office and residential environments.

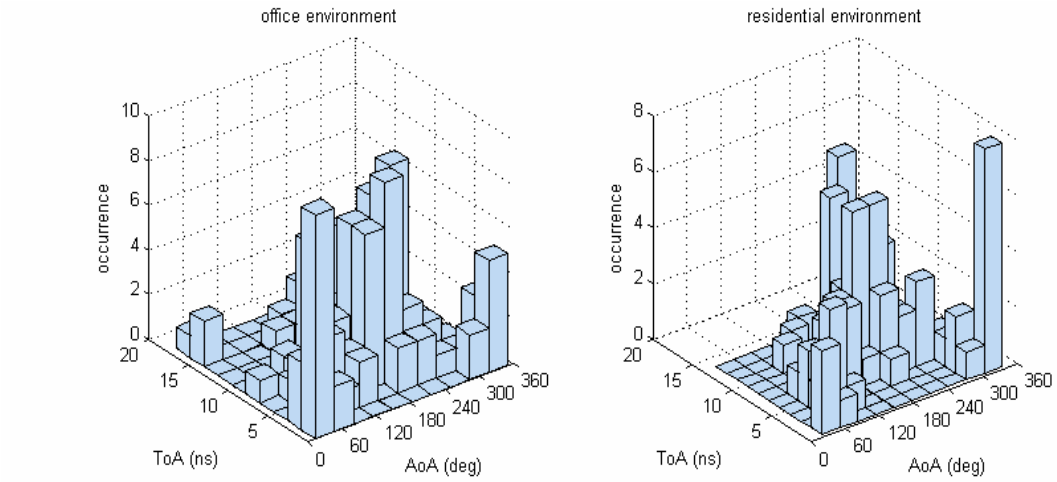

Figure 6. Joint histograms of the ToA and the AoA for office and residential environments.

Considering the similarity between office and residential environments, in the following analysis, we combine all the measured data for a sufficiently large sample space. Figure 7 shows a series of histograms, i.e., graphs of partial conditional AoA PDFs, $\{f(\theta_l|\tau_n), n = 0, 1, \cdots, N\text{-}1\}$. The value of K_n to generate each of these graphs are also shown on the plots. Note that at large

delay values (τ_n > 10 ns), fewer arrivals were observed. In order to obtain a good statistical representation, $\Delta\tau$ was chosen to be 10 ns to ensure a sufficiently large number of samples. Also note that graph (a) was generated differently: it was observed that rays with extremely short delays tend to arrive within the vicinity of 0°; so -180° to 180° notation was used and histogram of absolute AoA values was plotted (considering the symmetry). It can be seen that a Gaussian PDF centered at 180° with various standard deviations can provide a reasonably good match to the rest graphs. Note that although Figure 7b is more or less uniform, it can still be treated as a Gaussian distribution (still centered at 180°) with very large standard deviation. Therefore a modified Gaussian PDF is proposed to model $f(\theta_l|\tau_n)$:

$$f(\theta_l \mid \tau_n) = \begin{cases} \dfrac{1}{\sqrt{2\pi}\cdot\sigma_0}\exp\left[-\dfrac{(\theta_l-\theta_0)^2}{2\sigma_0^2}\right] & 0<\tau_n<\tau_0 \\ \dfrac{1}{\sqrt{2\pi}\cdot\sigma_{\theta_l|\tau_n}}\exp\left[-\dfrac{(\theta_l-180^\circ)^2}{2\sigma_{\theta_l|\tau_n}^2}\right] & \text{otherwise} \end{cases} \tag{5}$$

where τ_0, θ_0, and σ_0 are properly chosen constants (τ_0 = 2 ns, θ_0 = 30°, and σ_0 = 20° in our case), and $\sigma_{\theta_l|\tau_n}$ is the standard deviation conditioned upon τ_n and its variation can be approximated by the following fitting:

$$\sigma_{\theta_l|\tau_n}(\tau_n) = a\cdot\exp\left(-b\sqrt{\tau_n}\right) \tag{6}$$

where a and b are constants that can be estimated using a nonlinear least square regression method. Figure 8 show the extracted $\sigma_{\theta_l|\tau_n}$ from measured data and its least square fitting.

Much more measurements are needed for more accurate modeling of the joint PDF. At this time of designing this measurement campaign, no prior information was available on the multipath characteristics (AoA and ToA) at 60 GHz and with circular polarization.

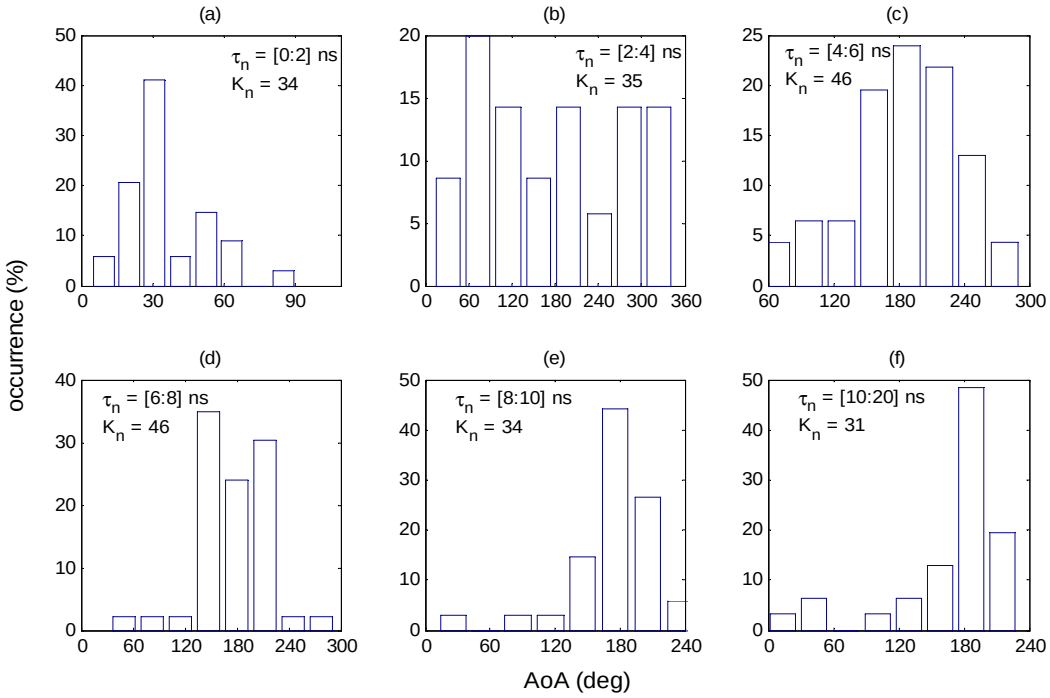

Figure 7. Partial conditional AoA PDFs for each delay step.

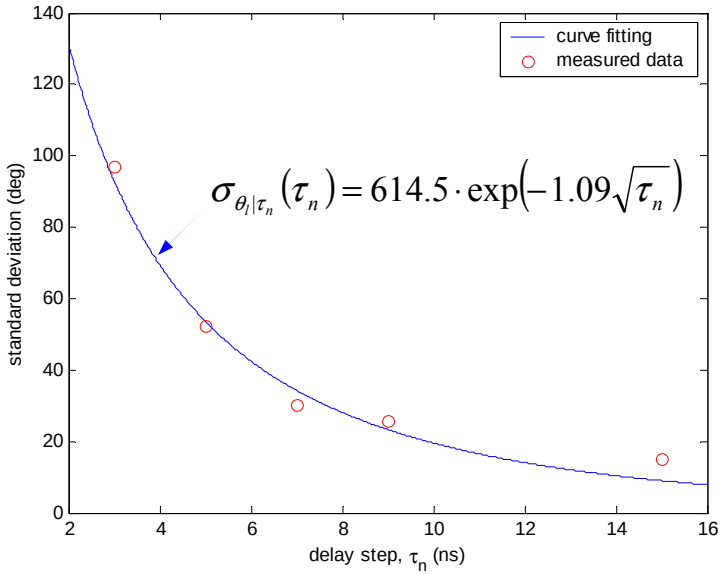

Figure 8. Standard deviation of the conditional AoA PDF as a function of delay step.

5.2 Power Delay Profile

The power delay profile (PDP) has been investigated experimentally in numerous studies and is therefore only shortly discussed here. In accordance with [4], [5], and [8-11], it is found that the average PDP is reasonably well modeled by a one-sided exponential decaying function, i.e.,

$$\overline{P}(t) \propto \begin{cases} P_0 \cdot \exp(-t/\gamma) & t > 0 \\ 0 & \text{otherwise} \end{cases} \tag{7}$$

where γ is the ray decay factor. Figure 9 shows the scatter plots of the normalized power versus the ToA for both office and residential environments with their estimated curves superimposed. The estimated parameters from the measured data was γ = 3.08 ns for the office environment and 2.56 ns for the residential environment and P_0 = -20.84 dB for the office environment and -22.11 dB for the residential environment.

One of the key components for small-scale fading is the amplitude statistics. Figure 10 shows the histogram of the normalized amplitude superimposed by an analytical Rayleigh distribution,

$$p(x) = \begin{cases} \dfrac{x}{\sigma} \cdot \exp\left(-\dfrac{x^2}{2\sigma^2}\right) & x > 0 \\ 0 & \text{otherwise} \end{cases} \tag{8}$$

where σ is chosen to be unity. We can see that the measured data fitted well to the Rayleigh distribution.

Another two parameters of practical interest are the mean delay, $\overline{\tau}$, and the RMS delay spread, τ_{RMS}, defined as [12]

$$\overline{\tau} = \frac{\int \tau \cdot P(\tau) d\tau}{\int P(\tau) d\tau} \text{ and } \tau_{\text{RMS}} = \sqrt{\frac{\int (\tau - \overline{\tau})^2 \cdot P(\tau) d\tau}{\int P(\tau) d\tau}}. \tag{9}$$

Note that both parameters are defined from a single PDP. Figure 11 shows the computed $\bar{\tau}$ and τ_{RMS} as well as the cumulative probability of the RMS delay for both office and residential environments. The results are consistent with those reported in [2].

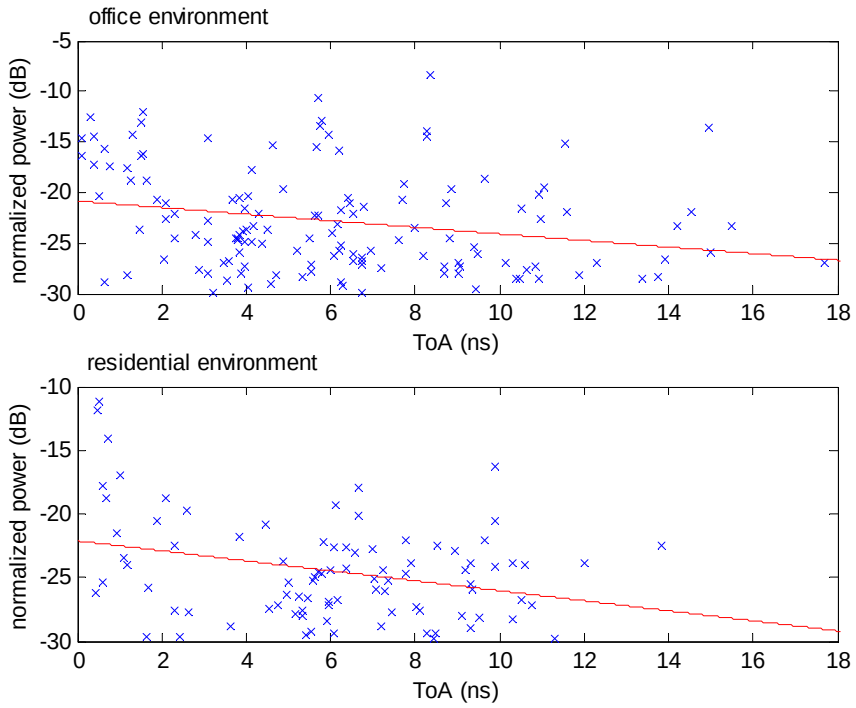

Figure 9. Scatter plots of the normalized power versus the ToA for office and residential environments.

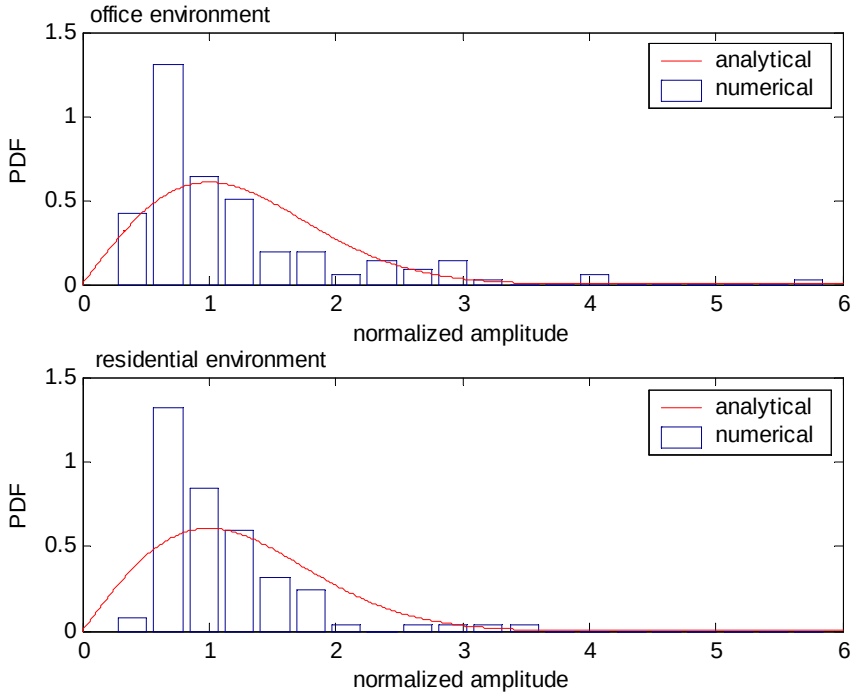

Figure 10. Amplitude distribution for office and residential environments

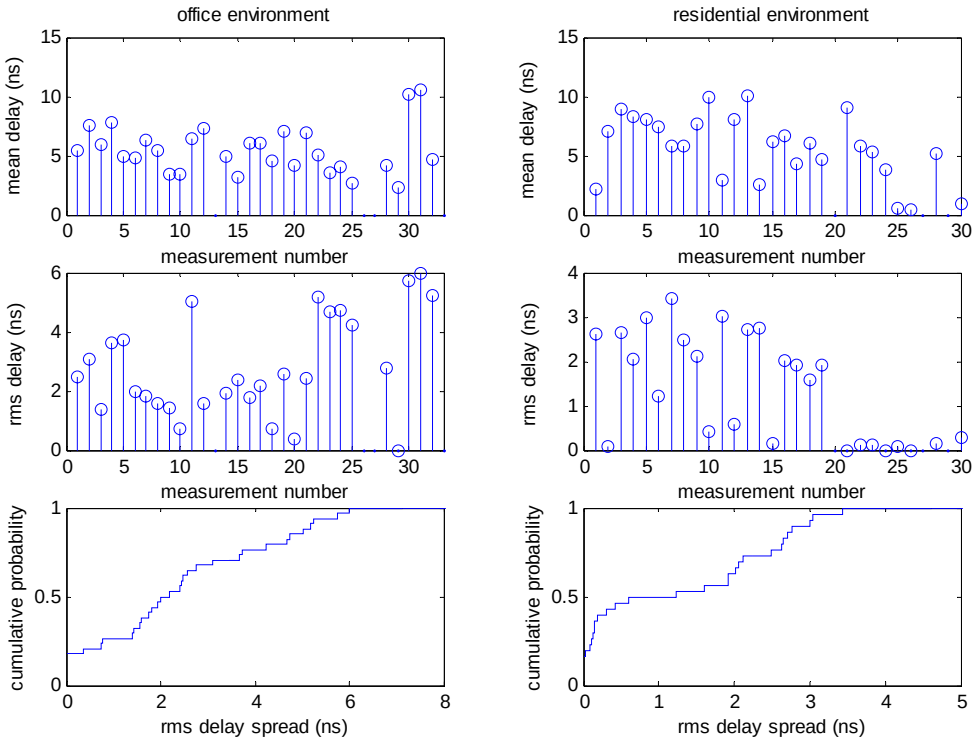

Figure 11. The mean delay and the RMS delay for office and residential environments.

5.3 Extracted Parameters

Channel parameters of all the proposed PDFs and PDP related parameters extracted from the measurement data for both office and residential environments are given in Table 2.

Table 2. Statistical Channel Parameters

Parameters			Values		Unit
			Office	Residential	
Ray Arrival Rate, 1/λ			2.11	2.29	ns
Ray Decay Factor, γ			3.08	2.56	ns
Conditional AoA PDF	τ_0		2		ns
	θ_0		30		deg
	σ_0		20		deg
	Mean		180		deg
	Standard Deviation	a	614.5		deg
		b	1.09		$ns^{-1/2}$
Mean Delay, $\bar{\tau}$			5.5	5.7	ns
RMS Delay Spread, τ_{RMS}			2.8	1.4	ns

6. Summary and Conclusions

A new statistical 60 GHz indoor channel model, which includes both ToA and AoA characteristics, has been proposed based on the measurement data collected in two different environments using circular polarized antennas. A time-domain measurement system that was used to simultaneously collect the temporal and spatial data was described. Data processing methods were outlined and statistical characteristics of the model parameters were presented. One of the major contributions of this paper is the thorough study of the joint PDF between the ToA and the AoA, which fully describes the temporal-spatial correlation properties of the multipath channel. To the best of the authors' knowledge, this paper is the first 60 GHz channel model based on circular polarized signals.

In general, the data presented here exhibited some general characteristics as the single-cluster S-V model and other modified S-V models. The ToAs in the measured data closely follow a single Poisson process, the mean amplitude of each arrival approximately follows a pattern of exponential decay, and the instantaneous amplitude follows a Rayleigh distribution. However there were some differences observed in the measured model parameters:

- About 50% (80%) of the arrivals have a relative power of -25 dB (-20 dB) or less compared to the LOS signal for both office and residential environments.
- No arrivals were observed within ±10° of the LOS direction for the office environment and ±20° for the residential environment.
- For both environments the ToA and the AoA are strong related. Rays arriving at the receiver with shorter (or longer) delays tend to have relatively smaller (or larger) AoAs. The conditional AoA PDFs are well described by a series of Gaussian distributions centered at 180° with various standard deviations except for those with extremely short delays.

7. Acknowledgement

The authors wish to thank Dr. Su-Khiong Yong and Dr. Tony Pollock for their helpful comments.

8. References

[1] T. Manabe, *et. al*., Multipath Measurement at 60 GHz for Indoor Wireless Communication Systems, *IEEE 44th Vehicular Technology Conference*, 905-909, June 1994.

[2] T. Manabe, *et. al*., Polarization Dependence of Multipath Propagation and High Speed Transmission Characteristics of Indoor Millimeter Channel at 60 GHz, *IEEE Transaction on Vehicular Technology*, Vol. **44**, No. **2**, 268-274, May 1995.

[3] K. Sato, *et. al*., Measurements of Reflection and Transmission of Office Building in the 60 GHz Band, *IEEE Transaction on Antennas and Propagation*, Vol. **45**, No. **12**, 1783-1792, December 1997.

[4] C. C. Chong, *et. al*., A New Statistical Wideband Spatio-Temporal Channel Model for 5 GHz Band WLAN Systems, *IEEE Journal on Selected Areas in Communications*, Vol. **21**, No. **2**, 139-150, February 2003.

[5] Q. H. Spencer, *et. al*., Modeling the Statistical Time and Angle of Arrival Characteristics of an Indoor Multipath Channel, *IEEE Journal on Selected Areas in Communications*, Vol. **18**, No. **3**, 347-359, March 2000.
[6] S. Haykin, Communications Systems (4th Edition), John Wiley & Sons, Inc., May 2000.
[7] A. A. M. Saleh and R. A. Valenzuela, **A S**tatistical Model for Indoor Multipath Propagation, *IEEE Journal on Selected Areas in Communications*, Vol. **5**, No. **2**, 128-137, February 1987.
[8] A. Davydov, *et. al*., Saleh-Valenzuela Channel Model Parameters for Library Environment, IEEE doc.: 802.15-06-0302-02-003c.
[9] T. Pollock, *et. al*., Office 60 GHz Channel Measurements and Model, IEEE doc.: 802.15-06-0316-00-003c.
[10] T. Pollock, *et. al*., Residential 60 GHz Channel Measurements and Model, IEEE doc.: 802.15-06-0317-00-003c.
[11] H. Sawada, *et. al*., LOS Office Channel Model Based on TSV Model, IEEE doc.: 802.15-06-0377-01-003c.
[12] T. S. Rappaport, Wireless Communications: Principles and Practice (2nd Edition), Prentice Hall Ptr., December 2001.